Supplementary Information (SI) for RSC Advances.

Supplementary Information

The novel quinoline derivative SKA-346 as a $K_{Ca}3.1$ channel selective activator

Brandon Han Siang Wong,[a,b] Heesung Shim,[c] Stephanie Shee Min Goay,[a,d] Seow Theng Ong,[a,d] Nur Ayuni Binte Muhammad Taib,[e] Kelila Xin Ye Chai,[e] Kerry Lim,[e] Dachuan Huang,[e] Choon Kiat Ong,[e,f] Thamil Selvan Vaiyapuri,[g] Yeong Cheng Cheah,[h] Yulan Wang,[h] Heike Wulff,[i] Richard D. Webster,[j] Vishalkumar G. Shelat,[a,k] and Navin Kumar Verma*[a]

[a.] Lee Kong Chian School of Medicine, Nanyang Technological University Singapore

[b.] Interdisciplinary Graduate Programme, NTU Institute for Health Technologies (HealthTech NTU), Nanyang Technological University Singapore

[c.] Physical and Life Sciences, Lawrence Livermore National Laboratory, Livermore, CA, USA

[d.] LKCMedicine-ICE Collaborative Platform, Lee Kong Chian School of Medicine, Nanyang Technological University, Singapore, Singapore.

[e.] Lymphoma Genomic Translational Research Laboratory, Division of Medical Oncology, and Laboratory of Cancer Epigenome, Division of Medical Sciences, National Cancer Centre Singapore

[f.] Duke-NUS Medical School, Singapore

[g.] MMD Lab, Institute of Molecular and Cell Biology, A*STAR, Singapore

[h.] Singapore Phenome Center, Lee Kong Chian School of Medicine, Nanyang Technological University Singapore

[i.] Department of Pharmacology, University of California Davis, CA, USA

[j.] School of Chemistry, Chemical Engineering and Biotechnology, Nanyang Technological University Singapore

[k.] Department of General Surgery, Tan Tock Seng Hospital, Singapore

* Corresponding author; **E-mail**: nkverma@ntu.edu.sg

A

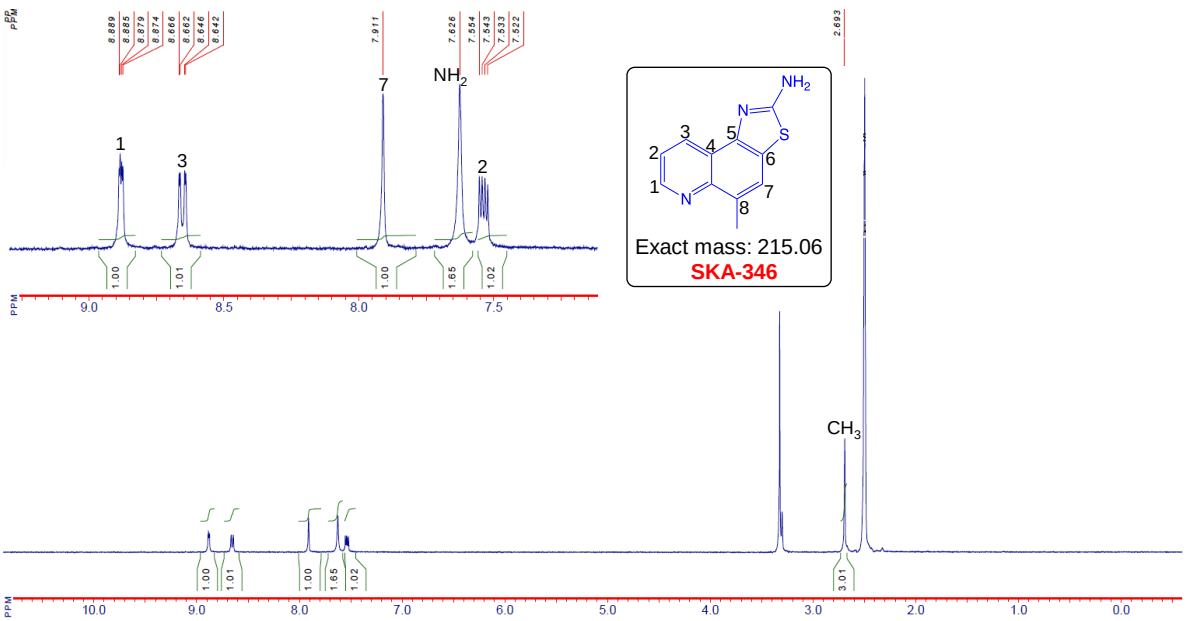

B

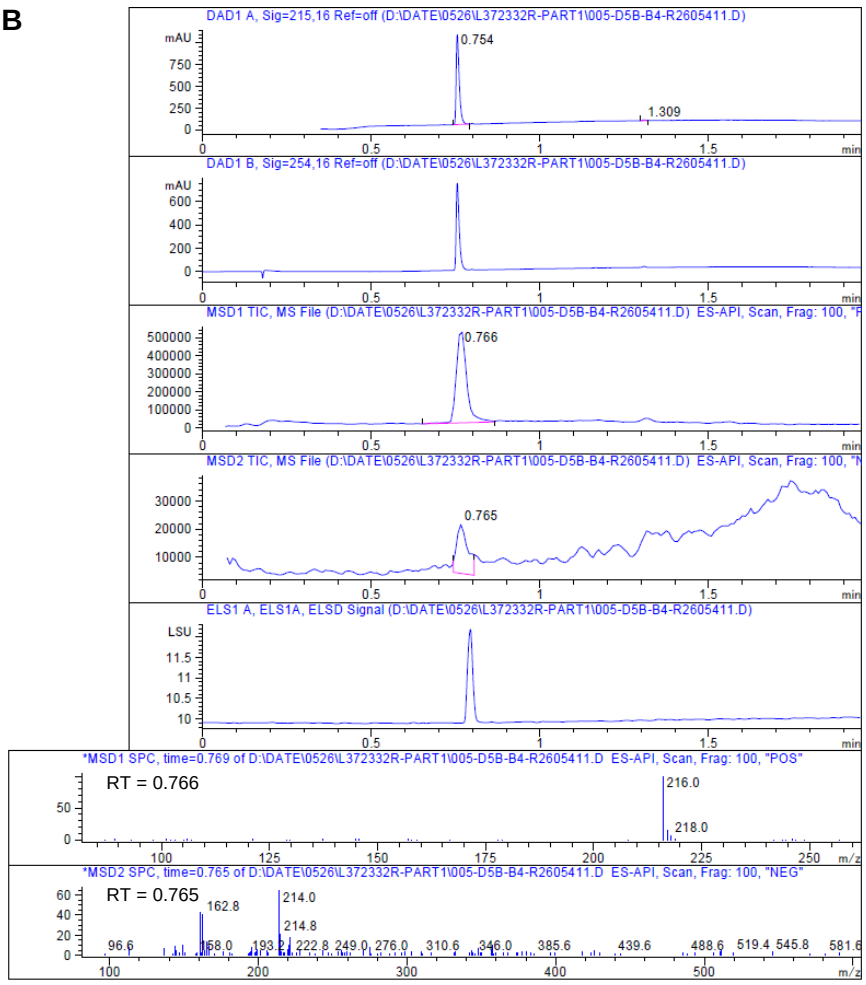

RT [min]	Area	Area %
0.754	667.008	99.27
1.309	6.20986	0.73

Supplementary Fig. 1. (A) ^{1}H NMR spectrum of SKA-346. Relevant signals are labelled. **(B)** LC-MS spectrum of SKA-346. RT, Retention time in minute.

A

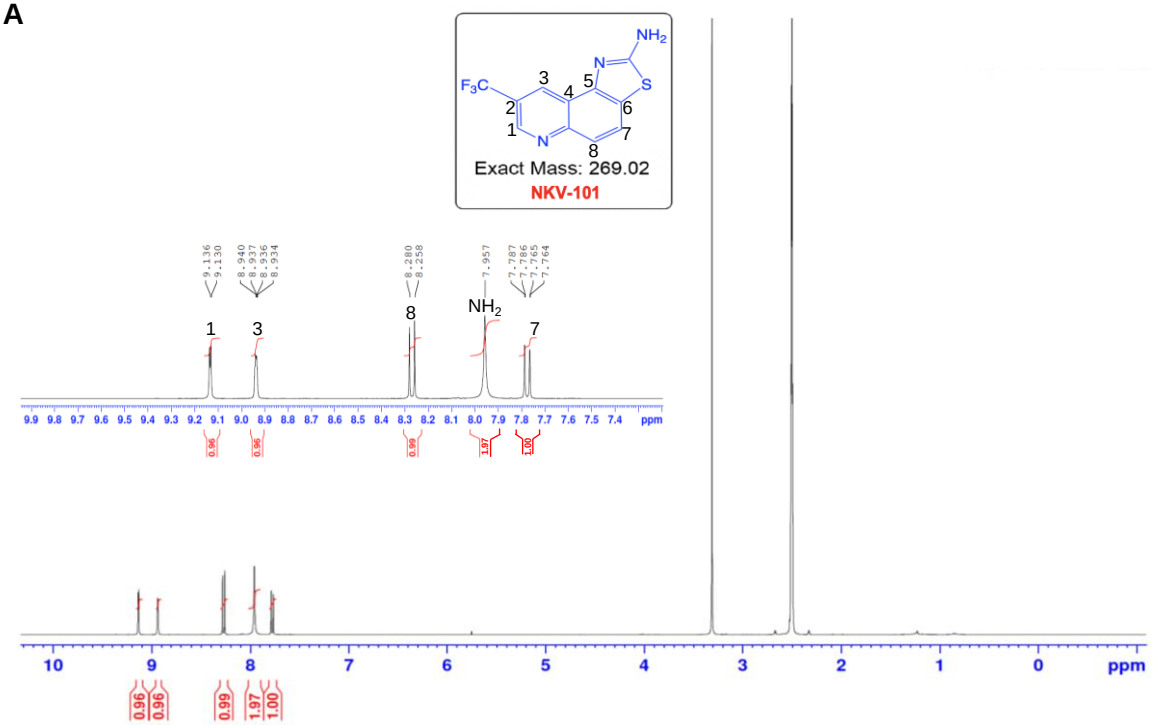

B

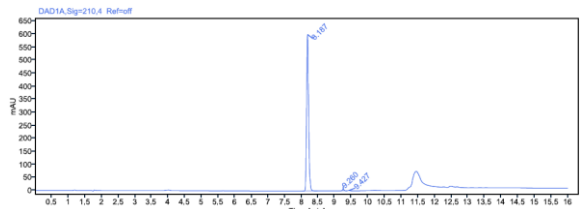

RT [min]	Area	Area %
8.187	2560	99.07
9.260	19	0.75
9.427	5	0.18

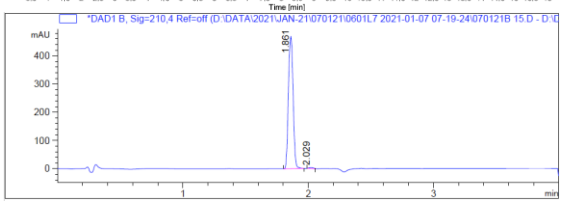

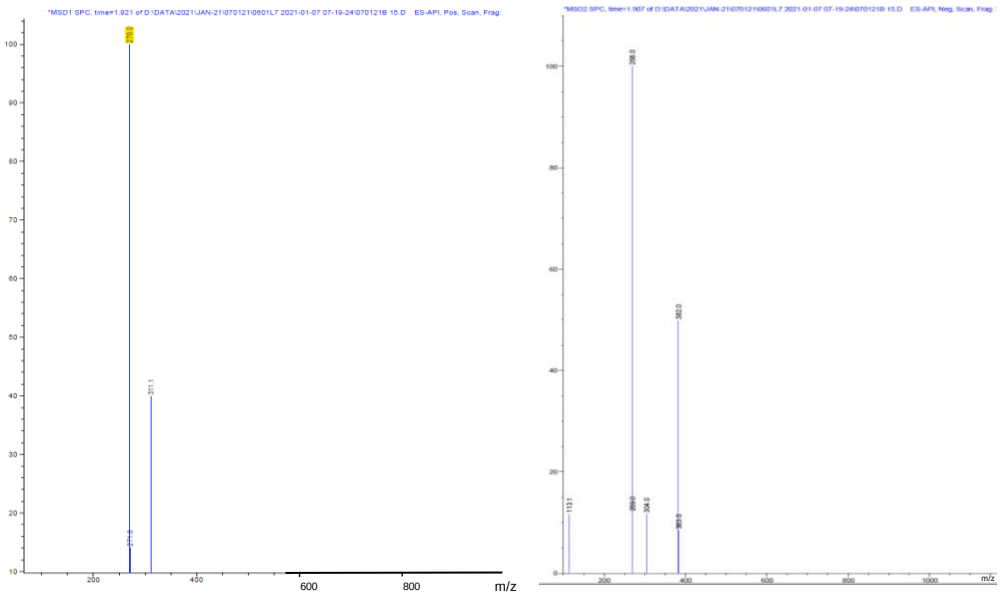

Supplementary Fig. 2. (A) ^{1}H NMR spectrum of NKV-101. Relevant signals are labelled. **(B)** LC-MS spectrum of NKV-101. RT, Retention time in minute.

A

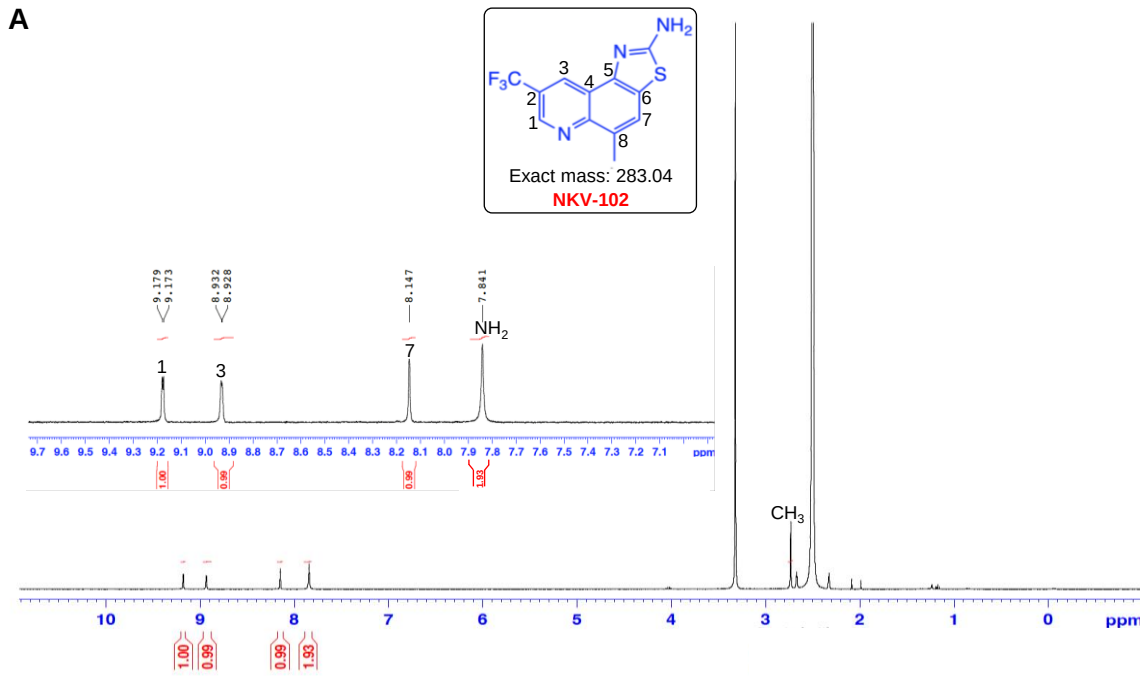

B

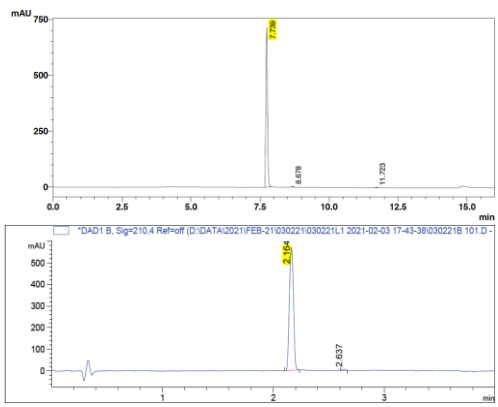

RT [min]	Area	Area %
7.739	2933784	99.209
8.678	14034	0.475
11.723	9356	0.316

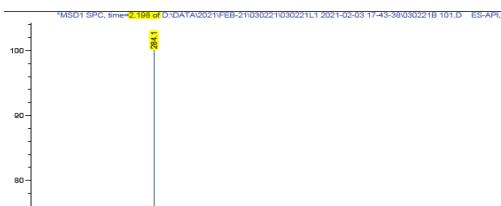

Supplementary Fig. 3. (A) ^{1}H NMR spectrum of NKV-102. Relevant signals are labelled. **(B)** LC-MS spectrum of NKV-102. RT, Retention time in minute.

A

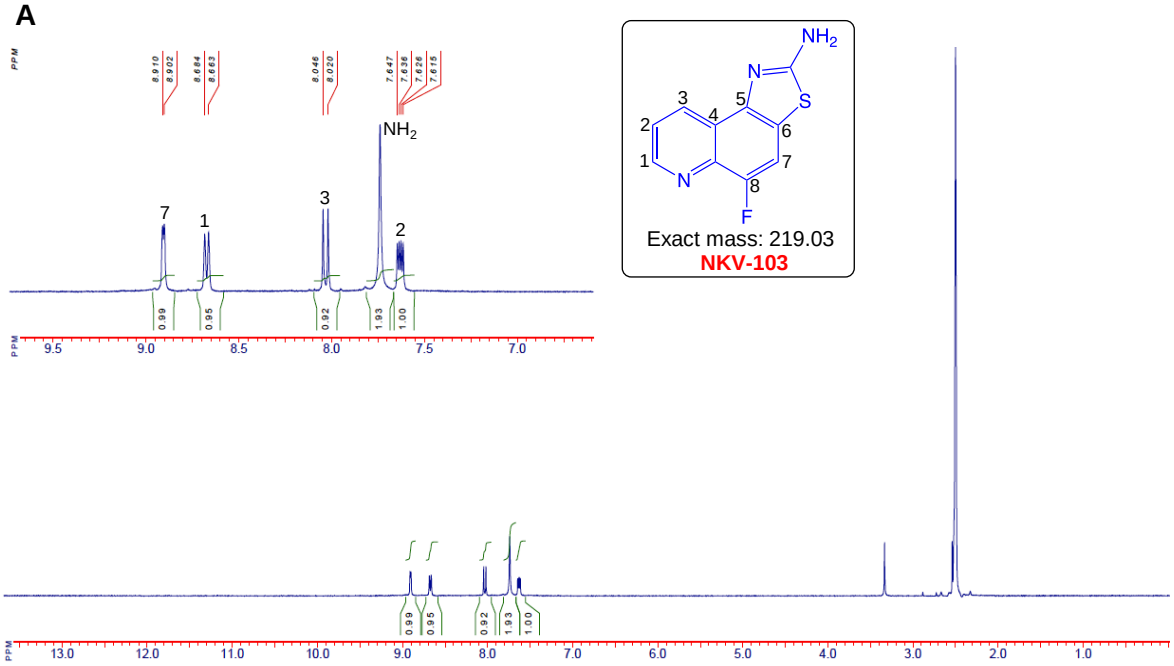

B

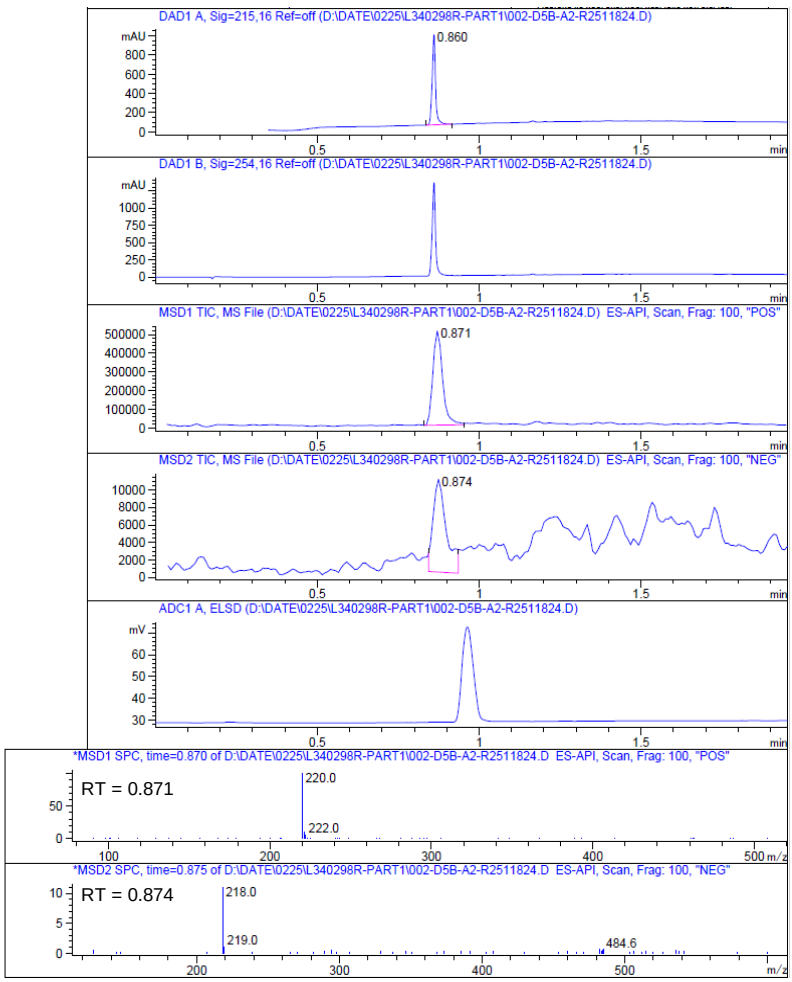

RT [min]	Area	Area %
0.860	682.48	100

Supplementary Fig. 4. (A) ^{1}H NMR spectrum of NKV-103. Relevant signals are labelled. **(B)** LC-MS spectrum of NKV-103. RT, Retention time in minute.

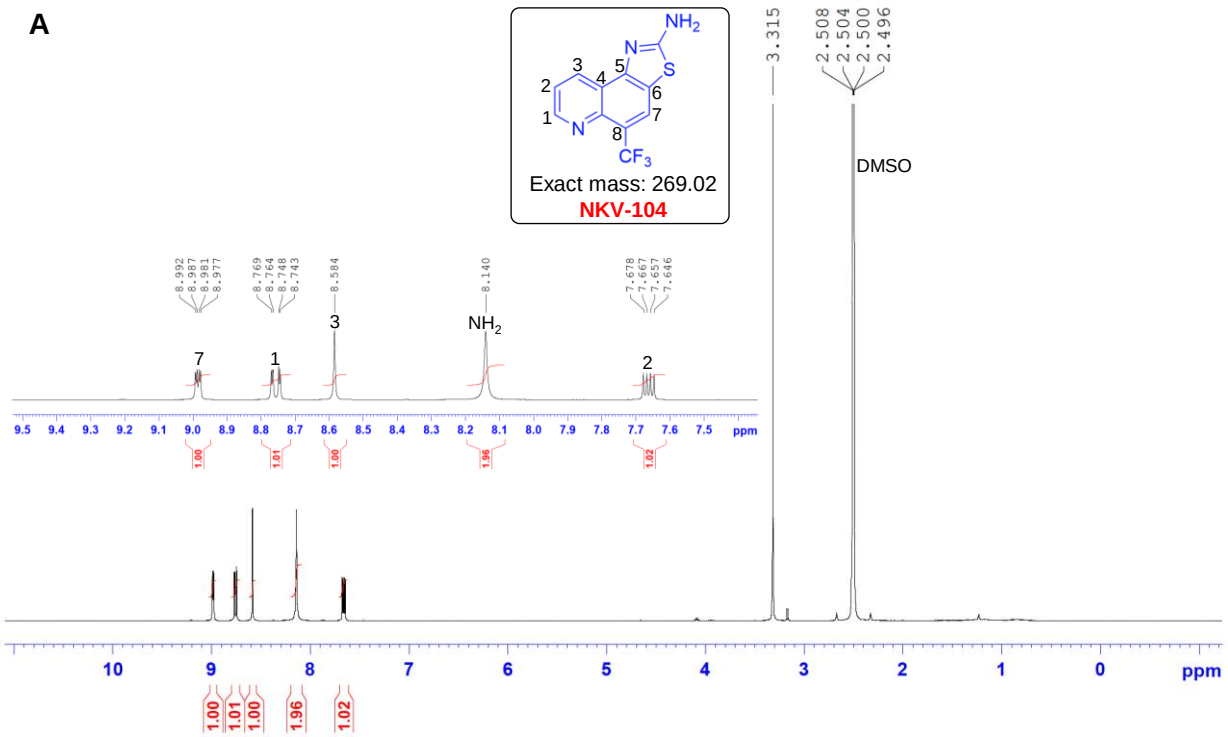

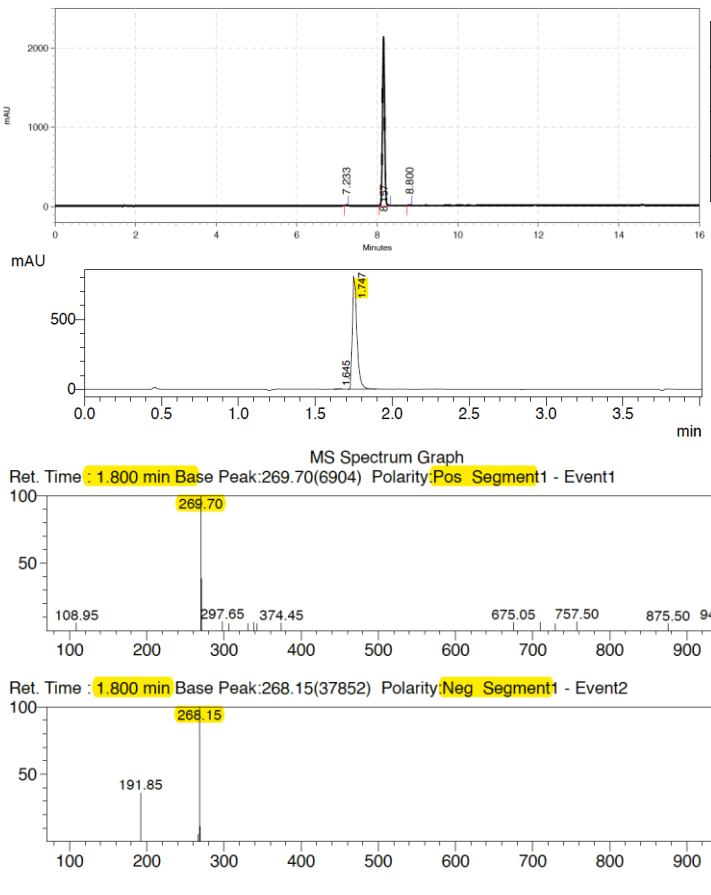

RT [min]	Area	Area %
7.23	7404	0.09
8.16	8029604	99.68
8.80	18077	0.22

Supplementary Fig. 5. (A) ^{1}H NMR spectrum of NKV-104. Relevant signals are labelled. **(B)** LC-MS spectrum of NKV-104. RT, Retention time in minute.

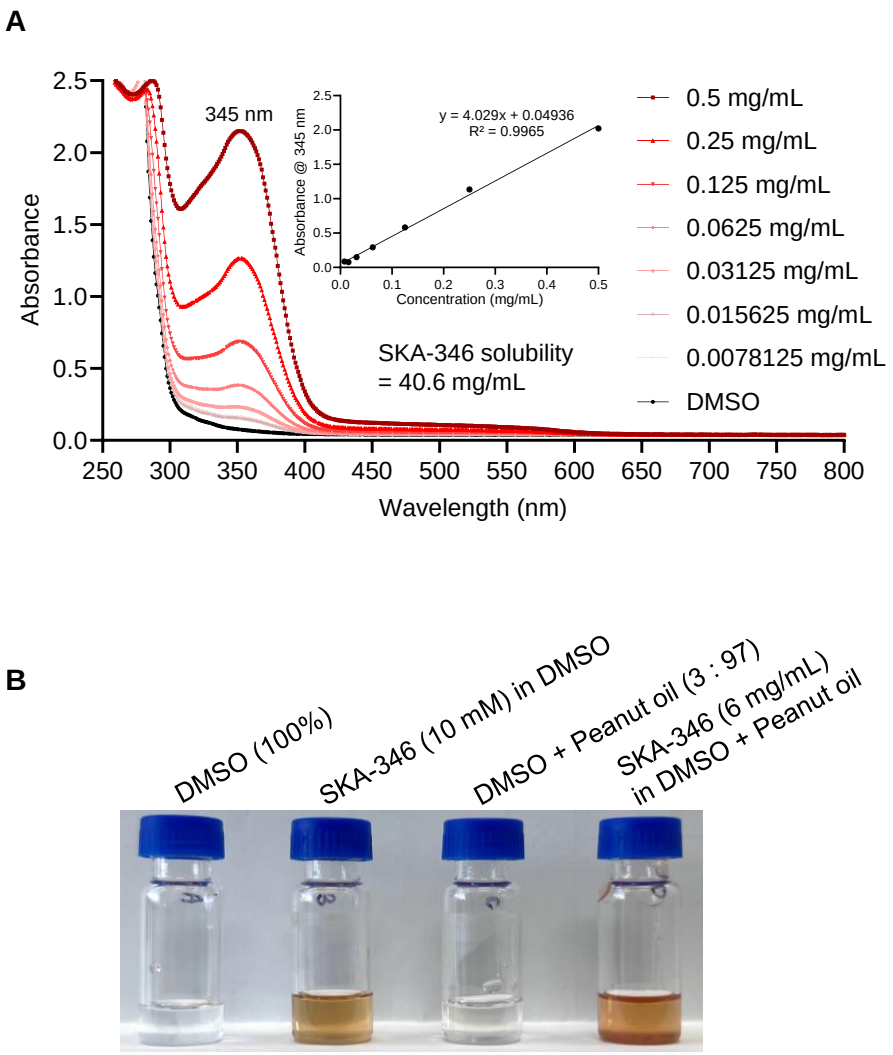

Supplementary Fig. 6. Solubility testing of SKA-346. **(A)** UV-Vis absorption spectra of SKA-346 at concentrations ranging from 0.007 to 0.5 mg/mL in DMSO. Inset shows calibration curve generated based on SKA-346 absorption peak at 345 nm. **(B)** Visual representation of SKA-346 solutions prepared in DMSO (10 mM) or DMSO + Peanut oil (3 : 97, 6 mg/mL) after left for 48 h at room temperature. SKA-346 was miscible in the solvents. Respective solvents are also shown.

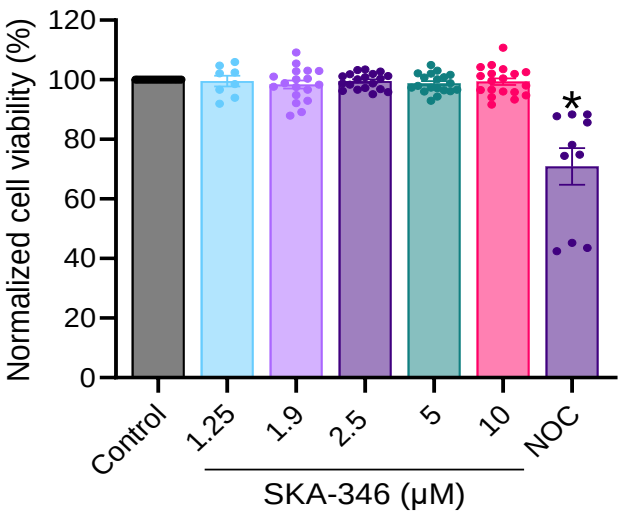

Supplementary Fig. 7. The viability (%) of human primary T-cells after treatment with increasing doses of SKA-346 (ranging from 1.25 to 10 μM) for 24 h. Cells were treated with nocodazole (NOC) as a kill control. Cell viability was determined by Promega CellTiter 96® AQ_{ueous} One Solution Cell Proliferation Assay (MTS) kit as per manufacturer's instructions. Data represents mean ± SEM of at least eight independent experiments. *p< 0.01 compared to untreated control.

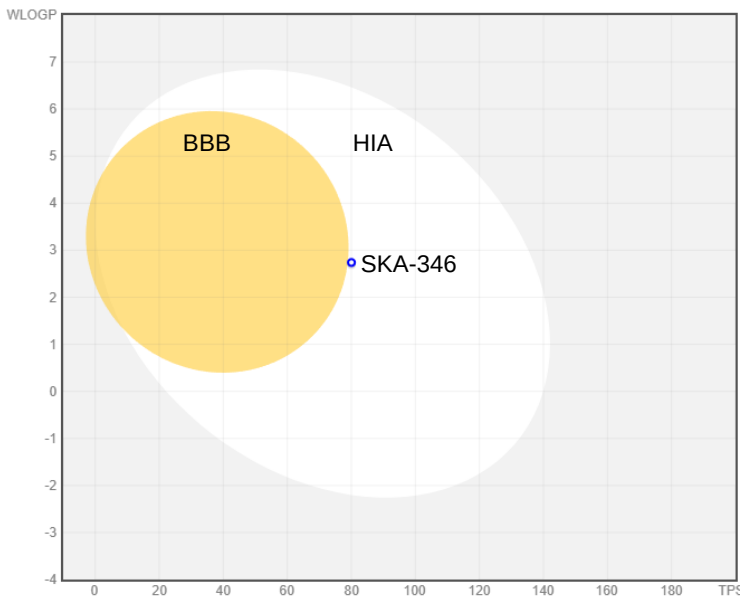

Supplementary Fig. 8. Boiled-egg model (obtained using SwissADME computational analysis) shows that SKA-346 does not penetrate the blood brain barrier (BBB). SKA-346 SMILES: CC1=CC2=C(N=C(N)S2)C2=C1N=CC=C2; HIA, human intestinal absorption.

A. Daina, O. Michielin and V. Zoete. SwissADME: a free web tool to evaluate pharmacokinetics, drug-likeness and medicinal chemistry friendliness of small molecules. *Sci Rep*., 2017, **7**, 42717.

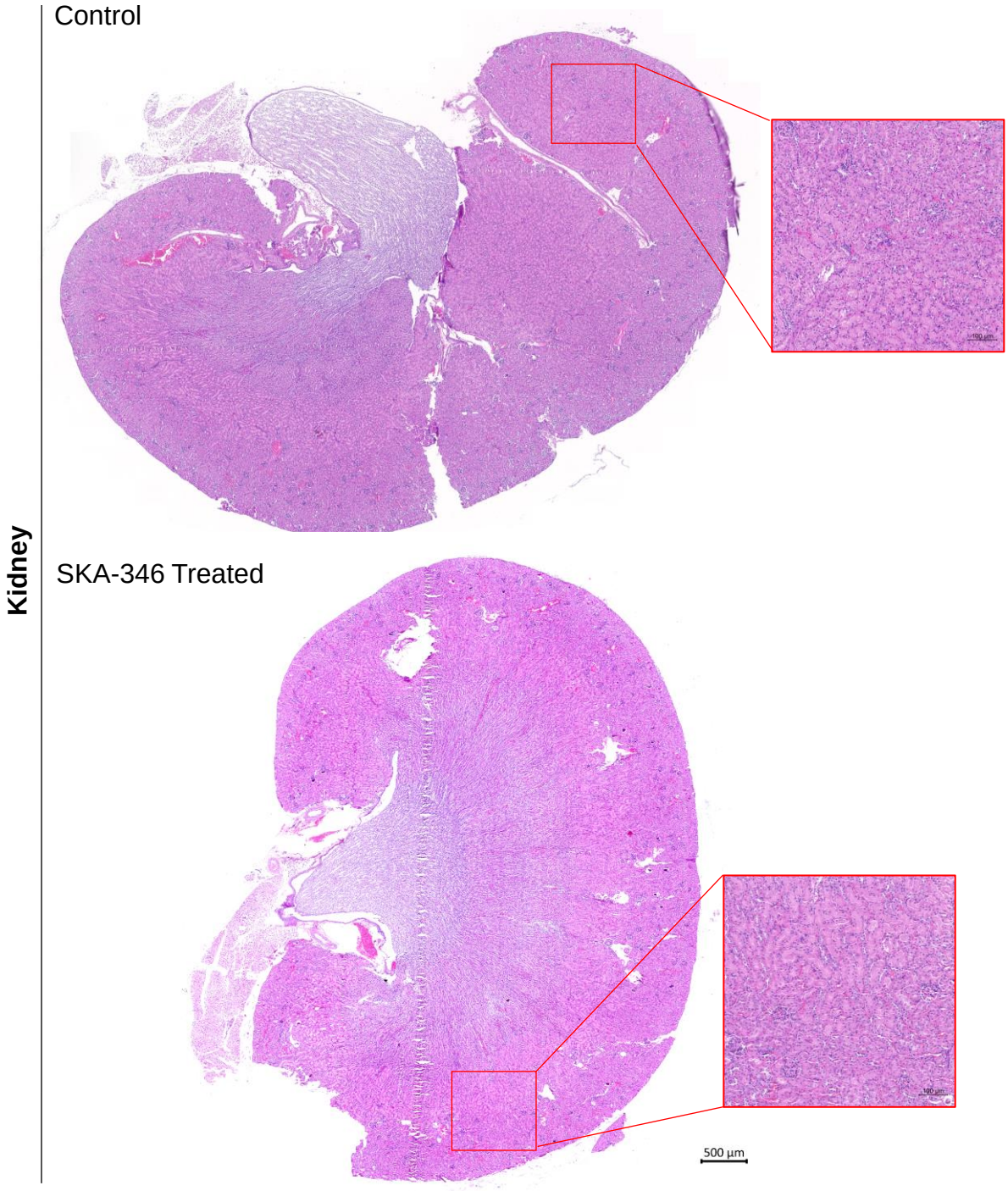

Supplementary Fig. 9. Histological sections of the kidney from C57BL/6 mice treated with vehicle control **(*top*)** or SKA-346 **(*bottom*)**. Tissue sections were stained with H&E. Magnified images of the designated tissue section areas are shown. Normal glomerular structures and hepatic architecture can be seen in the kidney sections of SKA-346 treated mice without any signs of necrosis, inflammation, or fibrosis. There is no detectable infiltration of mononuclear cells and neutrophils, vascular congestion in cortex and medulla area is absent. The kidney architecture is smooth and normal. The proximal and distal convoluted tubules are normal in both SKA-346 treated and vehicle control mice, indicating that SKA-346 does not cause renal toxicity.

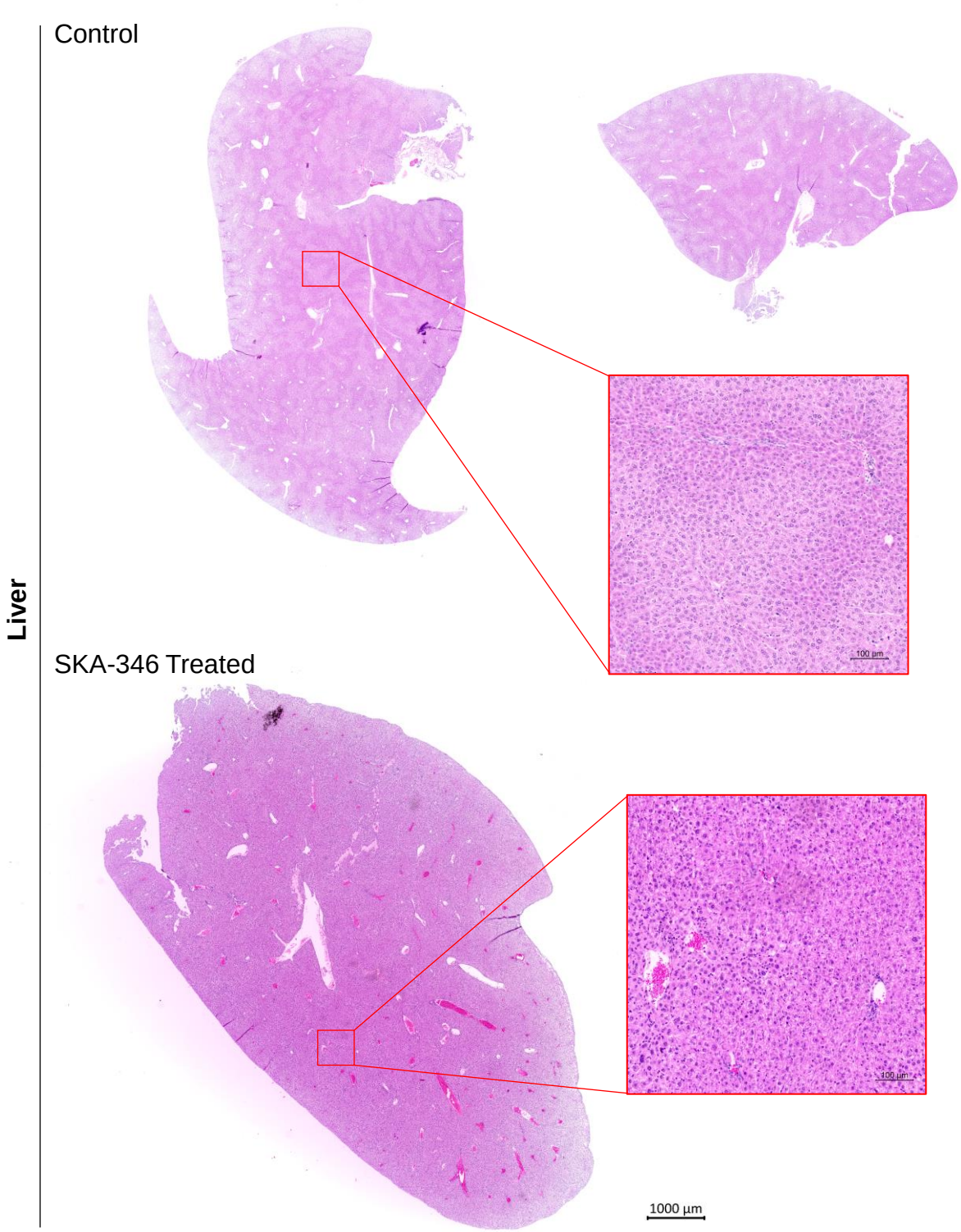

Supplementary Fig. 10. Histological sections of the liver from C57BL/6 mice treated with vehicle control **(*top*)** or SKA-346 **(*bottom*)**. Tissue sections were stained with H&E. Magnified images of the designated tissue section areas are shown. Liver histology of the SKA-346 treated animals is free of inflammatory cell infiltration and centrilobular and periportal area. Central vein and bile duct are intact and free from pathological lesion. Bile duct hyperplasia and vascular congestion are absent in both vehicle control and SKA-346 treated liver sections.

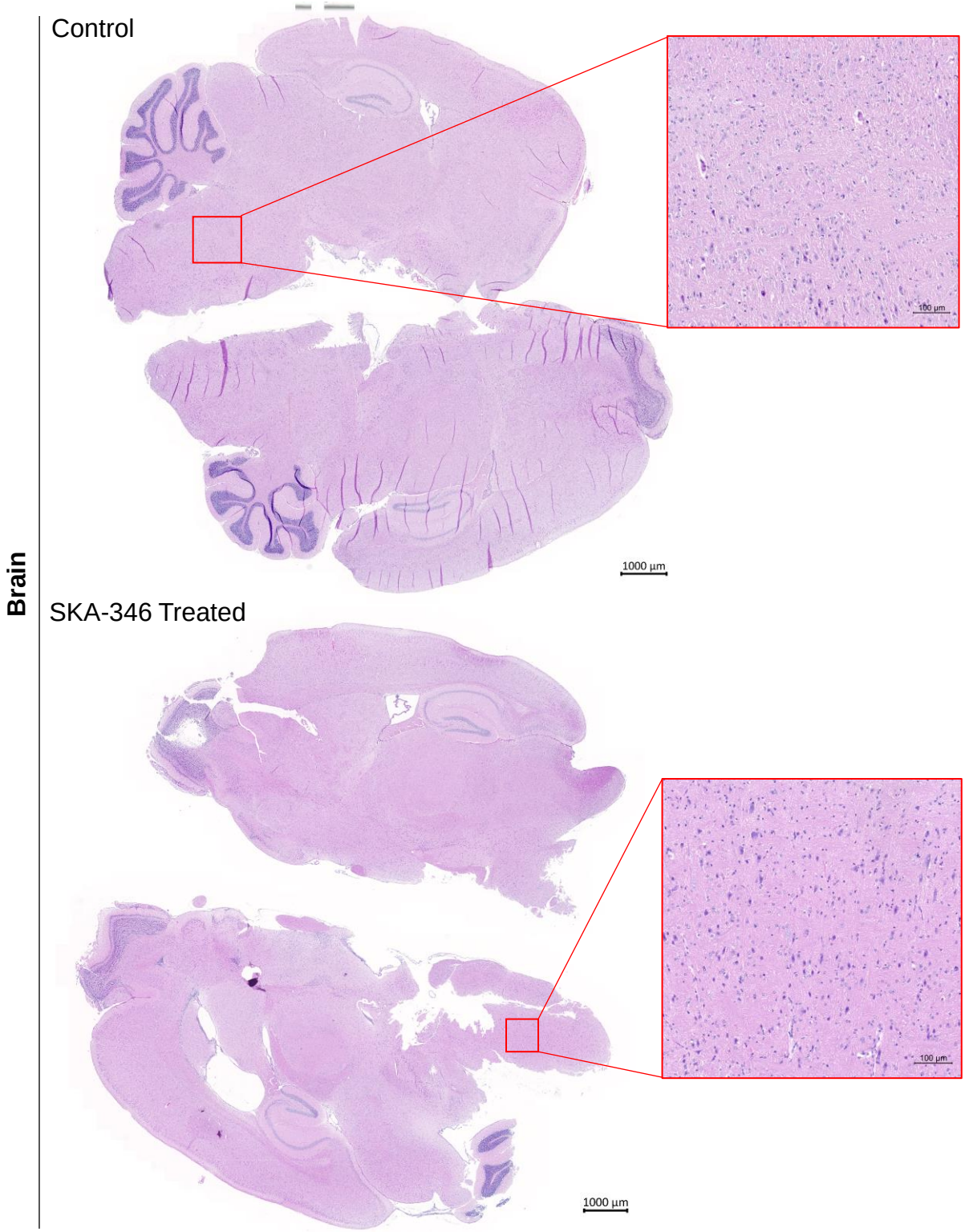

Supplementary Fig. 11. Histological sections of the brain from C57BL/6 mice treated with vehicle control **(*top*)** or SKA-346 **(*bottom*)**. Tissue sections were stained with H&E. Magnified images of the designated tissue section areas are shown. There is no evidence of neuronal damage in the cortex, olfactory bulb, and cerebellum. The hippocampus areas are intact and are free from necrosis with densely populated neuron cells.

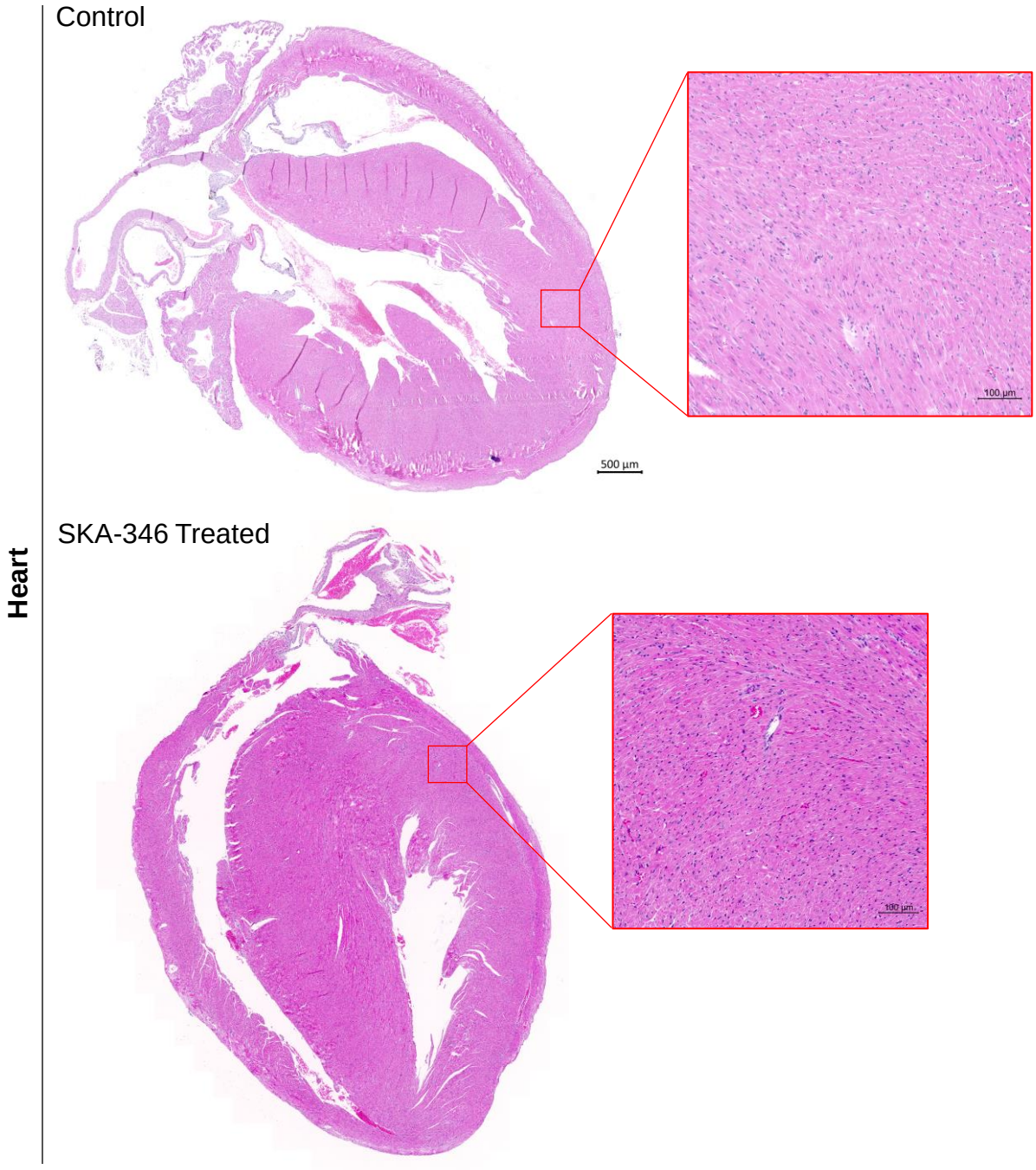

Supplementary Fig. 12. Histological sections of the heart from C57BL/6 mice treated with vehicle control **(*top*)** or SKA-346 **(*bottom*)**. Tissue sections were stained with H&E. Magnified images of the designated tissue section areas are shown. The heart sections display intact myocardial fibres with no indication of cardiotoxicity. Mild mineralization at epicardium of right ventricles can be observed in both SKA-346-treated and vehicle control mice, which are generally considered as background lesions. There is no vascular congestion in the right auricle.

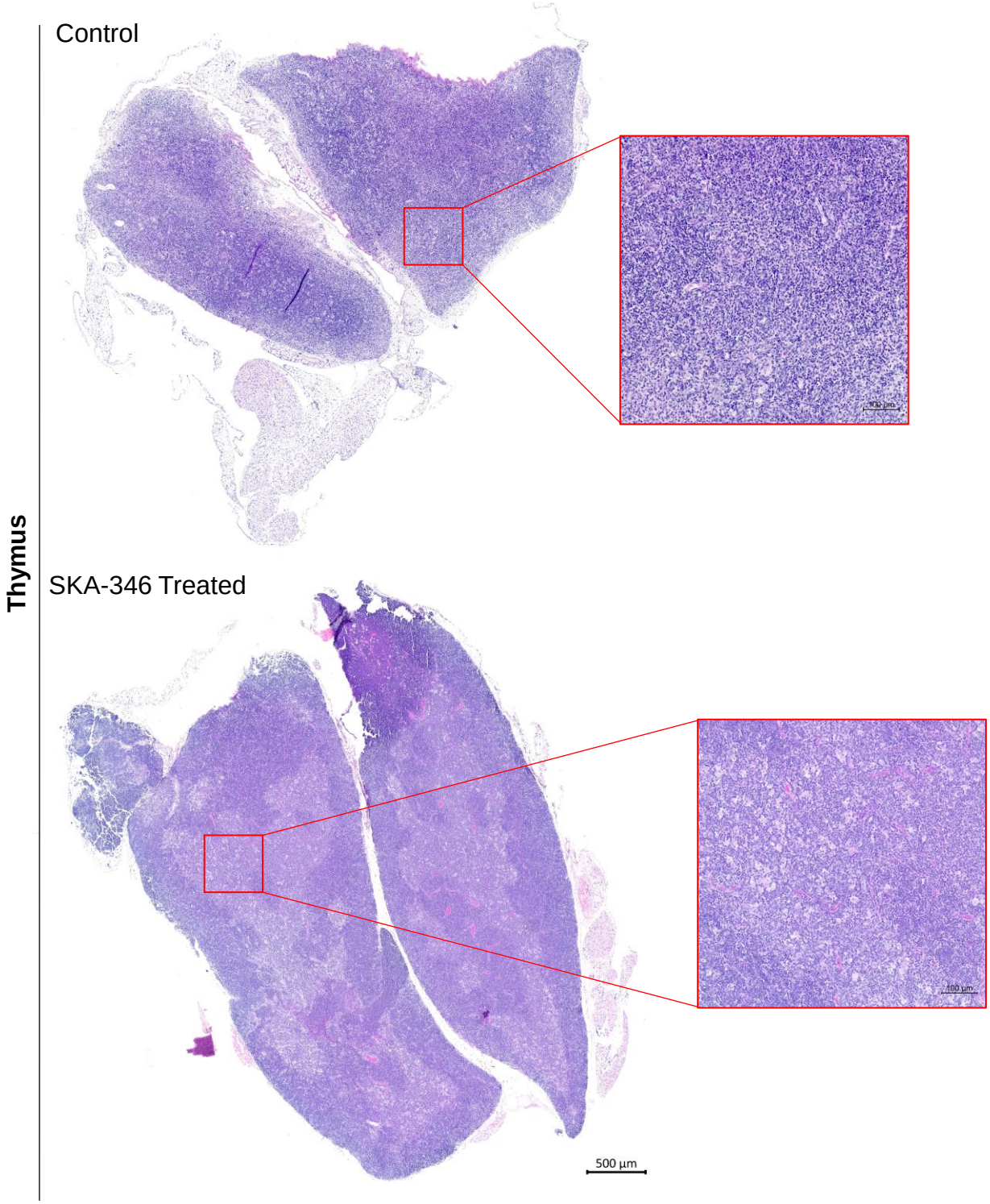

Supplementary Fig. 13. Histological sections of the thymus from C57BL/6 mice treated with vehicle control **(*top*)** and SKA-346 **(*bottom*)**. Tissue sections were stained with H&E. Magnified images of the designated tissue section areas are shown. Thymus sections show no signs of lymphoid depletion or histological abnormalities, indicating that SKA-346 does not adversely affect immune organs.

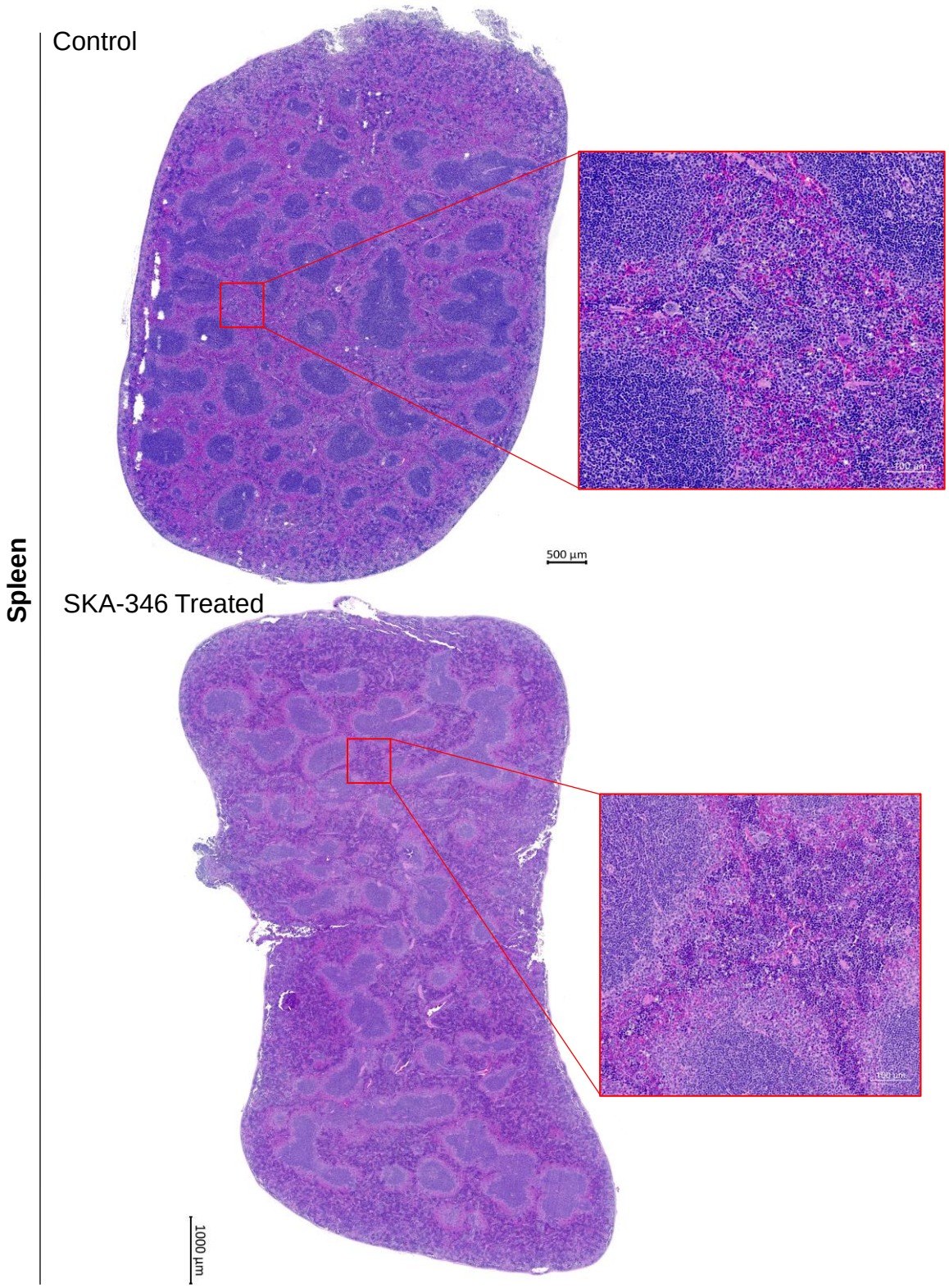

Supplementary Fig. 14. Histological sections of the spleen from C57BL/6 mice treated with vehicle control **(top)** or SKA-346 **(bottom)**. The sections were stained with H&E. Red boxes display a magnified image of the designated area of the tissue sections. Histopathological sections of spleen show diffuse hyperplasia of red pulp with mixture of cell lineages such as erythroid, myeloid series and few megakaryocytes can be noticed in spleen in both vehicle and SKA-346-treated mice. Some degree of extramedullary hematopoiesis is normally present in the rodent spleen, which can increase in response to hepatotoxic insult, anemia, bone marrow suppression, inflammation, tumours elsewhere in the body. Minimal vascular congestion and clear marginal zones are observed in both SKA-346 treated and control animals.

A

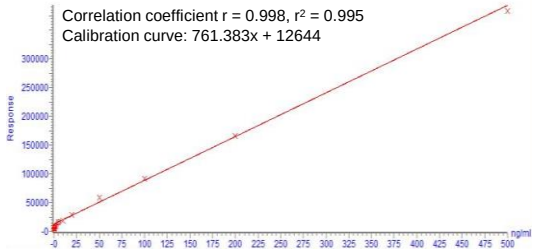

B

Retention time – 1.14 min

Timepoint (h)	0.25	0.5	1	2	4	8	24
Average peak response area (x 10^6)	1.21 ± 0.09	1.08 ± 0.12	1.15 ± 0.14	0.86 ± 0.10	0.79 ± 0.10	1.42 ± 0.31	0.02 ± 0.01
Average peak response height (x 10^6)	14.94 ± 0.97	13.69 ± 1.34	14.14 ± 1.43	10.68 ± 1.17	9.75 ± 1.14	4.85 ± 1.64	0.30 ± 0.13
Average peak concentration (x 10^3 ng/mL)	1.57 ± 0.12	1.41 ± 0.16	1.49 ± 0.19	1.11 ± 0.13	1.03 ± 0.13	0.45 ± 0.20	0.01 ± 0.01
Average peak signal to noise ratio	1.63 ± 0.34	1.91 ± 0.71	1.58 ± 0.59	1.47 ± 0.29	1.42 ± 0.31	1.02 ± 0.33	0.10 ± 0.05

Supplementary Fig. 15. (A) Standard concentration curve of SKA-346 ranging from 10 to 500 ng/mL. **(B)** LC-MS spectra of SKA-346 in BALB/c mice blood plasma samples (n=4, each time-point at 0.25 h, 0.5 h, 1 h, 2 h, 4 h, 8 h, and 24 h.

Supplementary Table 1. Pharmacokinetic parameters of SKA-346 in BALB/c mice blood plasma samples following 24 h post *i.p.* single dose administration

Parameters	Units	Estimate
N_Samples		7
Dose	mg	30
Rsq		0.9990666
Rsq_adjusted		0.99813321
Corr_XY		-0.99953319
No_points_lambda_z		3
Lambda_z	1/h	0.24422251
Lambda_z_intercept		9.3659546
Lambda_z_lower	h	4
Lambda_z_upper	h	24
HL_Lambda_z (t1/2)	h	2.838179
Span		7.046772
Tlag	h	0
Tmax	h	0.25
Cmax	ng/ml	6295.4
Cmax_D	kg*ng/ml/mg	209.8466
Tlast	h	24
Clast	ng/ml	32.7
Clast_pred	ng/ml	33.268614
AUClast	h*ng/ml	45487.063
AUClast_D	h*kg*ng/ml/mg	1516.2354
AUCall	h*ng/ml	45487.063
AUCINF_obs	h*ng/ml	45620.957
AUCINF_D_obs	h*kg*ng/ml/mg	1520.6986
AUC_%Extrap_obs	%	0.29349295
Vz_F_obs	ml/kg	2692.5959
Cl_F_obs	ml/h/kg	657.59252
AUCINF_pred	h*ng/ml	45623.285
AUCINF_D_pred	h*kg*ng/ml/mg	1520.7762
AUC_%Extrap_pred	%	0.29858121
Vz_F_pred	ml/kg	2692.4585
Cl_F_pred	ml/h/kg	657.55896
AUMClast	h*h*ng/ml	219263.62
AUMCINF_obs	h*h*ng/ml	223025.33
AUMC_%Extrap_obs	%	1.686674
AUMCINF_pred	h*h*ng/ml	223090.74
AUMC_%Extrap_pred	%	1.7155001
MRTlast	h	4.8203513
MRTINF_obs	h	4.8886596
MRTINF_pred	h	4.8898439